

Enhanced Light Trapping in Conformal CuO/Si Microholes Array Heterojunction for Self-Powered Broadband Photodetection

Chao Zhang, Bin Wang, Ruiyu Luo, Chunyan Wu[✉], Shirong Chen, Jigang Hu, *Member, IEEE*,
Chao Xie[✉], and Linbao Luo[✉], *Senior Member, IEEE*

Abstract—In this letter, we demonstrate the fabrication of a conformal CuO/Si microholes array heterojunction through the DC reactive magnetron sputtering from a high-purity Cu target. By using the monolayer graphene as the top electrode, the device served well as a self-powered *vis*-NIR photodetector, showing a high responsivity of 301.5 mA W^{-1} , specific detectivity of 7.96×10^{12} Jones and a fast response speed (rise time $9.9 \mu\text{s}$ and fall time $10 \mu\text{s}$) upon 530 nm illumination. Compared to its planar counterpart, the responsivity was remarkably enhanced over the broadband region. The underlying reason should be ascribed to the improved light trapping in the microholes *via* the longitudinal Fabry-Perot (F-P) cavity resonance, according to theoretical simulation by finite-difference time-domain (FDTD) solution. Such an effect gave rise to an enhanced light-matter interaction, leading to the improved photoresponse. This work also opens up an effective way for the on-chip high performance photodetection due to the well compatibility with the current complementary metal-oxide-semiconductor (CMOS) technology.

Index Terms—Fabry-Perot cavity resonance, light trapping, microholes array, broadband photodetection.

I. INTRODUCTION

BULK crystalline Si is a leading material for commercial visible light photodetectors due to its suitable bandgap ($\sim 1.12 \text{ eV}$), high carrier mobility, long-term stability, abundant material resources and the mature Si-based semiconductor manufacturing techniques [1]. However, the optical reflection loss of crystalline Si in visible region is up to 40% due to its high reflective index, which seriously limits the efficiency

of light harvesting and hinders the development of high-performance Si-based photoelectrical devices [2]. Researchers have been seeking for efficient strategies to achieve light trapping and subsequent absorption improvement and a wide range of photonics based phenomena such as the localized surface plasmon resonance (LSPR) [3] and metal gratings [4], [5] have been explored.

Si micro/nano structures, such as nanowire array [6], nanobowl array [7], micro pyramid array [8] and micro/nano hole array [9], [10], combine merits including suppressed light reflection, increased interfacial area, prolonged photocarrier lifetime and shortened carrier transit time. They offer another alternative way for efficient light harvesting towards optoelectronic applications. However, the vertical nanoscale textures such as nanowire and nanopillar are fragile and easily cracked, and can also hardly be applied in industrial practices due to the difficulty of subsequential conformal growth. Therefore, the hole geometry stands out and surpasses its counterparts in mechanical robustness [11], [12].

Herein, we propose the conformal CuO/Si microholes (MH) array heterojunction for self-powered *vis*-NIR photodetector, which exhibited remarkably enhanced photoresponse over a broadband wavelength region compared to its planar counterpart. Finite-difference time-domain (FDTD) solution revealed that the enhancement should be ascribed to the light trapping in the microholes *via* the longitudinal Fabry-Perot (F-P) cavity resonance, which led to the enhanced light-matter interaction and therefore the improved photocurrent.

II. EXPERIMENTS

The fabrication process of CuO/Si MH array heterojunction is shown in Fig. 1(a). Briefly, a circular window with diameter of 3 mm was defined on a pre-cleaned SiO₂ (300 nm)/Si (*n*⁺-type) substrate by an adhesive tape. A buffered oxide etch solution (BOE, HF:NH₄F:H₂O = 3 mL:6 g:10 mL) was used to remove the unprotected SiO₂ layer within the window. After that, a layer of Al film arrays with a diameter of 5 μm and a period of 10 μm were defined on the substrate through traditional photolithography and lift-off process, which was used as the metal mask for the following etching. The substrate was then loaded in an inductively coupled plasma (ICP-601) system for 20-min etching, using the high-purity gas SF₆ (40 sccm) as the etching gas. The RF power of the top and bottom electrodes were set to be 375 W and 75 W, respectively.

Manuscript received March 20, 2021; revised April 5, 2021; accepted April 6, 2021. Date of publication April 9, 2021; date of current version May 21, 2021. This work was supported in part by the Natural Science Foundation of China under Grant 62074048, Grant 51902078, Grant 61675062, Grant 62075053, and Grant U20A20216; and in part by the Fundamental Research Funds for the Central Universities under Grant PA2020GDKC0014, Grant PA2020GDKC0024, Grant JZ2020HGTB0051, Grant JZ2018HGXC0001, and Grant JZ2018HGPD0275. The review of this letter was arranged by Editor T.-Y. Seong. (Corresponding authors: Chunyan Wu; Jigang Hu; Linbao Luo.)

Chao Zhang, Bin Wang, Ruiyu Luo, Chunyan Wu, Shirong Chen, Jigang Hu, and Linbao Luo are with the School of Microelectronics, Hefei University of Technology, Hefei 230009, China (e-mail: cywu@hfut.edu.cn; hujigang@hfut.edu.cn; luolb@hfut.edu.cn).

Chao Xie is with the School of Electronics and Information Engineering, Anhui University, Hefei 230601, China.

Color versions of one or more figures in this letter are available at <https://doi.org/10.1109/LED.2021.3072042>.

Digital Object Identifier 10.1109/LED.2021.3072042

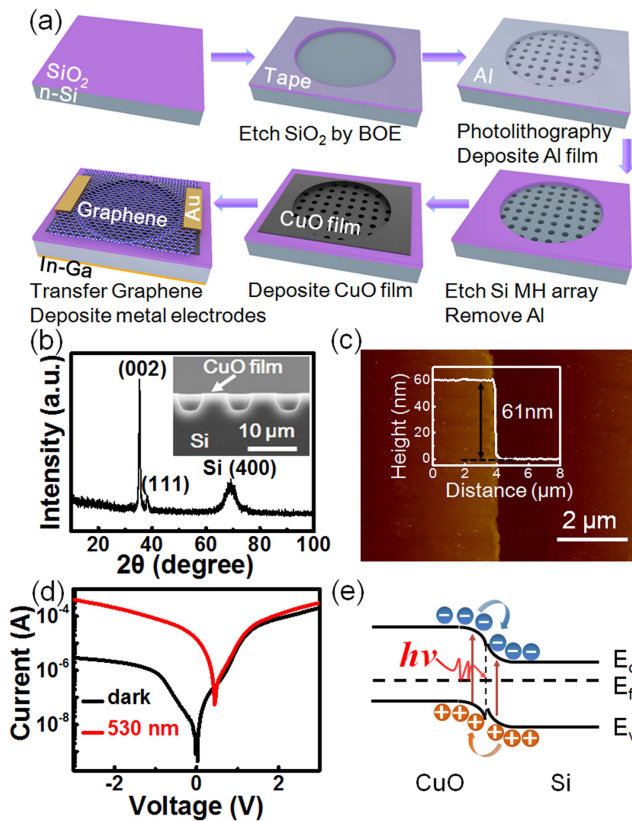


Fig. 1. (a) Schematic illustration of the step-wise process for the fabrication of CuO/Si MH array heterojunction. (b) XRD pattern of the obtained CuO film. Inset shows the cross-sectional SEM image of the heterojunction. (c) AFM image and the height profile of CuO film deposited on planar Si. (d) I - V curves of the device in the dark and upon 530 nm illumination (light intensity: 36.2 mW cm^{-2}) curve in a semilogarithmic scale. (e) The energy band diagram of the CuO/Si heterojunction upon light illumination at zero bias.

After removal of Al film, CuO film was deposited *via* DC reactive magnetron sputtering for 80 s using a high-purity Cu target and the mixed gas of Ar (20 sccm) and O₂ (15 sccm) as the working gas [13], [14]. For the effective collection of photo-generated carriers, a layer of chemical vapor deposition (CVD)-grown monolayer graphene was transferred to the top of the heterojunction through the poly(methylmethacrylate) (PMMA)-assisted wet transfer method.

Optoelectronic characterization of the CuO/Si MH array heterojunction was carried out on a semiconductor characterization system (Keithley 4200-SCS) equipped with a broadband monochromator (SP 2150, Princeton Co.). Laser diodes with different wavelengths were also used as illumination sources, whose power intensity were carefully calibrated using a power meter (Thorlabs GmbH., PM 100D) before measurement. The transient photoresponse was characterized in a lab-built system, in which a signal generator (Tektronix, TDS2022B) was employed to connect the laser diode to produce pulsed light of varied frequencies, and an oscilloscope (Tektronix, TDS2012B) was used to record the electrical signal.

III. RESULTS AND DISCUSSION

As we can see from the inset in Fig. 1(b), the periodic MH array shows an inverted taper shape with the upper hole diameter of $\sim 5 \mu\text{m}$, the bottom hole diameter of $\sim 3 \mu\text{m}$ and

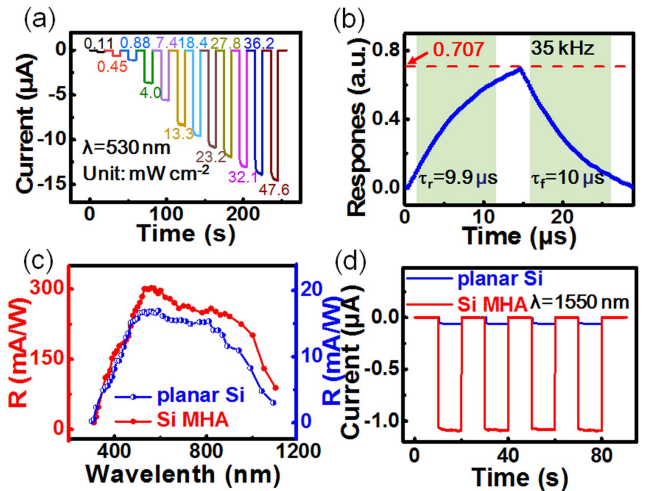


Fig. 2. (a) Time response of the CuO/Si MH array heterojunction photodetector upon 530 nm illumination with different light intensity at zero bias. (b) A single magnified photoresponse curve at the frequency of 35 kHz to calculate the response time. (c) Spectral response of the CuO/Si MH array heterojunction photodetector and its planar Si counterpart in the range of 300-1100 nm. (d) Time response of the two devices upon 1550 nm illumination.

the hole depth of $\sim 4 \mu\text{m}$. X-ray diffraction (XRD) pattern shown in Fig. 1(b) can be well indexed to monoclinic CuO (JCPDS Card No. 45-0937), revealing the pure phase of obtained CuO film. AFM images proved that the obtained CuO nanofilm has a relatively smooth surface with the root mean square roughness of about 2 nm and thickness of about 61 nm (Fig. 1(c)). Fig. 1(d) presents the current-voltage (I - V) curves of the CuO/Si MH array heterojunction in the dark and upon light illumination. A typical rectifying behavior with a rectification ratio of 70 at $\pm 3 \text{ V}$ can be observed under dark. When illuminated by 530 nm light with an intensity of 36.2 mW cm^{-2} , the heterojunction displayed a remarkable photovoltaic characteristic with an open-circuit voltage (V_{OC}) of 0.44V and a short-circuit current (I_{SC}) of $15.2 \mu\text{A}$. The photovoltaic characteristics of the device can be well understood by the energy band diagram of the CuO/Si heterojunction (Fig. 1(e)). A built-in electric field with the direction from Si to CuO would be formed at the heterojunction interface when p -type CuO film was in contact with n -type Si. Upon light illumination by incident light with photon energy higher than the bandgap of CuO or Si, the electron-hole pairs generated within or near the depletion region would be rapidly separated toward opposite directions, giving rise to the generation of photocurrent at zero bias. The photovoltaic behavior of the CuO/Si MH array heterojunction enables its application as a self-driven photodetector which can work without external electrical power supply.

Fig. 2(a) plots the time-dependent photoresponse of the device upon 530 nm illumination with varied light intensity at zero bias. Apparently, the photocurrent rose from $0.17 \mu\text{A}$ to $14.35 \mu\text{A}$ with the increase of light intensity from 0.11 mW cm^{-2} to 47.6 mW cm^{-2} , which could be ascribed to the increased concentration of photogenerated carriers at an evaluated light intensity. The heterojunction photodetector also presented a good photo-switching property with excellent reproducibility. Both the rise and fall edges were very steep,

indicating the rapid separation and collection of photoexcited electrons and holes in the heterojunction. The transient photoresponse revealed that the -3 dB frequency of the device was located at about 35 kHz, showing the rise time τ_r and fall time τ_f of 9.9 and 10 μ s, respectively. Notably, the response speed was comparable to that of Si-based Schottky devices, such as Cu/Si NW array [6] and BLG/Si NH array [9]. Furthermore, responsivity (R), specific detectivity (D^*) and external quantum efficiency (EQE) were calculated to be 301.5 mA W $^{-1}$, 7.96 $\times 10^{12}$ Jones and 70.5%, respectively, at the light intensity of 1.94 μ W cm $^{-2}$ under zero bias according to the following equations [15]:

$$R = \frac{I_p - I_d}{SP_{in}} \quad (1)$$

$$D^* = \frac{R}{(2qI_d/S)^{1/2}} \quad (2)$$

$$EQE = R\left(\frac{hc}{q\lambda}\right) \quad (3)$$

where q , h , c , λ and S denote the elementary electronic charge, the Planck's constant, the speed of light, the incident light wavelength and the effective illuminated area (about 0.07 cm 2 for this device), respectively. The responsivity and specific detectivity were much better than those of CuO/Si NW array heterojunction, in which Si NW array was coated by CuO nanoflakes synthesized through solution method [16]. We believe that this should be ascribed to the benign heterojunction interface formed through the conformal growth. Fig. 2(c) presents the spectral response of the CuO/Si MH array and the CuO/planar Si heterojunction photodetectors in the range of 300-1100 nm at a fixed light intensity (~ 2 μ W cm $^{-2}$). Apparently, the CuO/Si MH array heterojunction showed a remarkably enhanced photoresponse than its planar counterpart over the broad wavelength range from visible to NIR region. The device also exhibited a stable and repeatable response to 1550 nm incident light, which was far beyond the absorption limit of intrinsic CuO and Si (Fig. 2(d)). This is probably attributed to the red shift of the absorption region and the increased absorption coefficient of CuO in the NIR region arising from the inevitable defects formed during the deposition process [17]. Clearly, the photoresponse of the CuO/Si MH array surpassed that of its planar counterpart by at least one order of magnitude over the broadband range of 300-1550 nm.

To gain the physical insight for the significantly enhanced photoresponse of the CuO/Si MH array heterostructure, FDTD solution was adopted to calculate the electrical field distribution. During simulation, the structural parameters of the model are extracted from the SEM image of the experiment (inset in Fig. 1(b)). The top monolayer graphene was modeled as an effective surface conductivity sheet, whose permittivity can be expressed as the formula $\epsilon_g = 1 + i\sigma_g/(\omega\epsilon_0t)$ [18], where ω , ϵ_0 and σ_g are the angular frequency, the permittivity of vacuum, and the surface conductivity of graphene. Periodic boundary conditions were applied in horizontal direction to simulate an infinite area in the X and Y directions, and the perfectly matched layer (PML) boundary conditions were set on the top/bottom sides. In order to ensure the accuracy of the calcu-

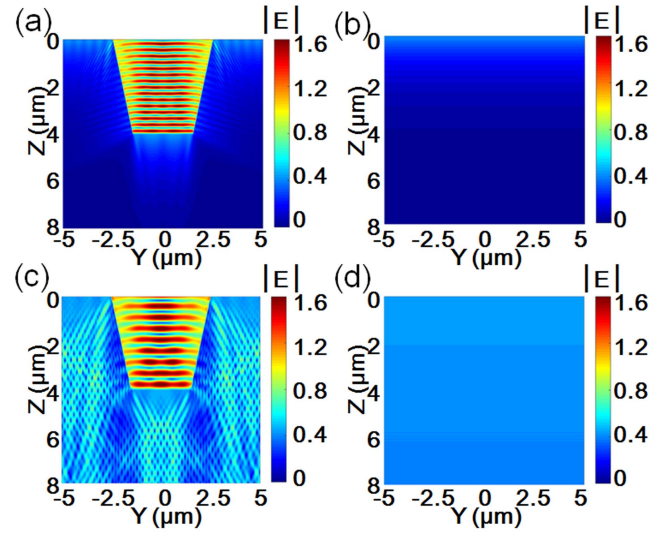


Fig. 3. The simulated $|E|$ field intensity distributions of YOZ plane for (a) the CuO/Si MH array structure and (b) the planar Si structure at the wavelength of 530 nm. (c)-(d) are the same as those in (a)-(b) but at the wavelength of 970 nm. All structures are normally illuminated by the light with the y-polarization. The unit of $|E|$ field intensity is V/m.

lation results, the spatial mesh grids are set as $X = Y = 20$ nm and $Z = 5$ nm. Due to the symmetry of rotation in the periodic Si holes, there will be no difference in the optical response between the x- and the y-polarization. Herein, light is incident from the top with the polarization along y-direction. Compared with the planar structure (shown in Fig. 3(b)), the simulated $|E|$ field of the designed MH arrays exhibited a typical standing wave patterns in the hole due to the F-P cavity resonance in Z-direction (shown in Fig. 3(a)). For the case of 970 nm, the remarkable F-P resonance enhanced standing-wave fields can also be observed in the hole, just with a lower resonance order (Fig. 3(c)). Notably, the intensity of optical fields inside silicon at 970 nm was higher than at 530 nm. This was ascribed to the lower optical absorption loss of Si over the longer wavelength region [19]. Therefore, simulation results revealed that the designed MH array configuration can effectively trap the incident light *via* the longitudinal F-P cavity resonance over a broad wavelength range. This led to an enhanced light-matter interaction and therefore gave rise to the improved photoresponse of the device.

IV. CONCLUSION

In summary, a conformal CuO/Si MH array heterojunction has been fabricated through the DC reactive magnetron sputtering. By using the monolayer graphene as the top electrode, the heterojunction functioned well as a self-powered broadband photodetector, showing a high responsivity, specific detectivity and fast response speed of 301.5 mA W $^{-1}$, 7.96 $\times 10^{12}$ Jones and 9.9/10 μ s (the rise/fall time) upon 530 nm illumination, respectively. FDTD solution revealed that the enhancement in photoresponse should be ascribed to the improved light-matter interaction in the hole *via* the longitudinal F-P cavity resonance. The well compatibility with the complementary metal-oxide-semiconductor (CMOS) technology also facilitates the on-chip integration of the high performance photodetection.

REFERENCES

- [1] X. Gong, M. Tong, Y. Xia, W. Cai, J. S. Moon, Y. Cao, G. Yu, C.-L. Shieh, B. Nilsson, and A. J. Heeger, "High-detectivity polymer photodetectors with spectral response from 300 nm to 1450 nm," *Science*, vol. 325, no. 5948, pp. 1665–1667, Sep. 2009, doi: [10.1126/science.1176706](https://doi.org/10.1126/science.1176706).
- [2] Y. M. Song, Y. Z. Xie, V. Malyarchuk, J. Xiao, I. Jung, K.-J. Choi, Z. Liu, H. Park, C. Lu, R.-H. Kim, R. Li, K. B. Crozier, Y. Huang, and J. A. Rogers, "Digital cameras with designs inspired by the arthropod eye," *Nature*, vol. 497, pp. 95–99, May 2013, doi: [10.1038/nature12083](https://doi.org/10.1038/nature12083).
- [3] J.-A. Huang and L.-B. Luo, "Low-dimensional plasmonic photodetectors: Recent progress and future opportunities," *Adv. Opt. Mater.*, vol. 6, no. 8, Apr. 2018, Art. no. 1701282, doi: [10.1002/adom.201701282](https://doi.org/10.1002/adom.201701282).
- [4] Y. Park, E. Drouard, O. E. Daif, X. Letartre, P. Viktorovitch, A. Fave, M. Lemiti, and C. Seassal, "Absorption enhancement using photonic crystals for silicon thin film solar cells," *Opt. Exp.*, vol. 17, no. 16, pp. 14312–14321, Aug. 2009, doi: [10.1364/OE.17.014312](https://doi.org/10.1364/OE.17.014312).
- [5] J. Hu, W. Xie, J. Chen, L. Zhou, W. Liu, D. Li, and Q. Zhan, "Strong hyperbolic-magnetic polaritons coupling in an hBN/Ag-grating heterostructure," *Opt. Exp.*, vol. 28, no. 15, pp. 22095–22104, Jul. 2020, doi: [10.1364/OE.398182](https://doi.org/10.1364/OE.398182).
- [6] C.-Y. Wu, Z.-Q. Pan, Y.-Y. Wang, C.-W. Ge, Y.-Q. Yu, J.-Y. Xu, L. Wang, and L.-B. Luo, "Core-shell silicon nanowire array-Cu nanofilm Schottky junction for a sensitive self-powered near-infrared photodetector," *J. Mater. Chem. C*, vol. 4, no. 46, pp. 10804–10811, Oct. 2016, doi: [10.1039/c6tc03856e](https://doi.org/10.1039/c6tc03856e).
- [7] J. He, P. Gao, M. Liao, X. Yang, Z. Ying, S. Zhou, J. Ye, and Y. Cui, "Realization of 13.6% efficiency on 20 μm thick Si/organic hybrid heterojunction solar cells via advanced nanotexturing and surface recombination suppression," *ACS Nano*, vol. 9, no. 6, pp. 6522–6531, Jun. 2015, doi: [10.1021/acs.nano.5b02432](https://doi.org/10.1021/acs.nano.5b02432).
- [8] F.-X. Liang, X.-Y. Zhao, J.-J. Jiang, J.-G. Hu, W.-Q. Xie, J. Lv, Z.-X. Zhang, D. Wu, and L.-B. Luo, "Light confinement effect induced highly sensitive, self-driven near-infrared photodetector and image sensor based on multilayer PdSe₂/pyramid Si heterojunction," *Small*, vol. 15, no. 44, Sep. 2019, Art. no. 1903831, doi: [10.1002/sml.201903831](https://doi.org/10.1002/sml.201903831).
- [9] L. Zeng, C. Xie, L. Tao, H. Long, C. Tang, Y. H. Tsang, and J. Jie, "Bilayer graphene based surface passivation enhanced nano structured self-powered near-infrared photodetector," *Opt. Exp.*, vol. 23, no. 4, pp. 4839–4846, Feb. 2015, doi: [10.1364/OE.23.004839](https://doi.org/10.1364/OE.23.004839).
- [10] P. Lv, X. Zhang, X. Zhang, W. Deng, and J. Jie, "High-sensitivity and fast-response graphene/crystalline silicon Schottky junction-based near-IR photodetectors," *IEEE Electron Device Lett.*, vol. 34, no. 10, pp. 1337–1339, Oct. 2013, doi: [10.1109/LED.2013.2275169](https://doi.org/10.1109/LED.2013.2275169).
- [11] K.-Q. Peng, X. Wang, L. Li, X.-L. Wu, and S.-T. Lee, "High-performance silicon nanohole solar cells," *J. Amer. Chem. Soc.*, vol. 132, no. 20, pp. 6872–6873, May 2010, doi: [10.1021/ja910082y](https://doi.org/10.1021/ja910082y).
- [12] X. Wang, Z. Yang, P. Gao, X. Yang, S. Zhou, D. Wang, M. Liao, P. Liu, Z. Liu, S. Wu, J. Ye, and T. Yu, "Improved optical absorption in visible wavelength range for silicon solar cells via texturing with nanopyramid arrays," *Opt. Exp.*, vol. 25, no. 9, pp. 10466–10472, May 2017, doi: [10.1364/OE.25.010466](https://doi.org/10.1364/OE.25.010466).
- [13] N. G. Elfadill, M. R. Hashim, K. M. Chahrouh, M. A. Qaeed, and W. Chunsheng, "The influence of oxygen pressure on the growth of CuO nanostructures prepared by RF reactive magnetron sputtering," *J. Mater. Sci., Mater. Electron.*, vol. 25, no. 1, pp. 262–266, Jan. 2014, doi: [10.1007/s10854-013-1581-8](https://doi.org/10.1007/s10854-013-1581-8).
- [14] J. Li, Y. Zhao, H. Wang, Y. Zhou, M. Zhang, H. Fu, B. Zhang, X. Li, and F. Yang, "Effects of oxygen flow rates on the physical characteristics of magnetron sputtered CuO films," *Vacuum*, vol. 168, Oct. 2019, Art. no. 108811, doi: [10.1016/j.vacuum.2019.108811](https://doi.org/10.1016/j.vacuum.2019.108811).
- [15] C. Xie, P. You, Z. Liu, L. Li, and F. Yan, "Ultrasensitive broadband phototransistors based on perovskite/organic-semiconductor vertical heterojunctions," *Light, Sci. Appl.*, vol. 6, no. 8, Aug. 2017, Art. no. e17023, doi: [10.1038/lsa.2017.23](https://doi.org/10.1038/lsa.2017.23).
- [16] Q. Hong, Y. Cao, J. Xu, H. Lu, J. He, and J.-L. Sun, "Self-powered ultrafast broadband photodetector based on p-n heterojunctions of CuO/Si nanowire array," *ACS Appl. Mater. Interface*, vol. 6, no. 23, pp. 20887–20894, Nov. 2014, doi: [10.1021/am5054338](https://doi.org/10.1021/am5054338).
- [17] C.-Y. Wu, J.-W. Kang, B. Wang, H.-N. Zhu, Z.-J. Li, S.-R. Chen, L. Wang, W.-H. Yang, C. Xie, and L.-B. Luo, "Defect-induced broadband photodetection of layered γ -In₂Se₃ nanofilm and its application in near infrared image sensors," *J. Mater. Chem. C*, vol. 7, no. 37, pp. 11532–11539, Sep. 2019, doi: [10.1039/C9TC04322E](https://doi.org/10.1039/C9TC04322E).
- [18] A. Vakil and N. Engheta, "Transformation optics using graphene," *Science*, vol. 332, no. 6035, pp. 1291–1294, Jun. 2011, doi: [10.1126/science.1202691](https://doi.org/10.1126/science.1202691).
- [19] C. Schinke, P. C. Peest, J. Schmidt, R. Brendel, K. Bothe, M. R. Vogt, I. Kröger, S. Winter, A. Schirmacher, S. Lim, H. T. Nguyen, and D. MacDonald, "Uncertainty analysis for the coefficient of band-to-band absorption of crystalline silicon," *AIP Adv.*, vol. 5, no. 6, Jun. 2015, Art. no. 067168, doi: [10.1063/1.4923379](https://doi.org/10.1063/1.4923379).